21st IMEKO TC4 International Symposium and
19th International Workshop on ADC Modelling and Testing
Understanding the World through Electrical and Electronic Measurement
Budapest, Hungary, September 7-9, 2016

Experimental comparison of two mathematical models for Analog-to-Information Converters

Pasquale Daponte, Luca De Vito, Grazia Iadarola, Mariangela Iovini, Sergio Rapuano

Department of Engineering, University of Sannio,
piazza Roma, 21, 82100 Benevento, Italy
{daponte, devito, grazia.iadarola, mariangela.iovini, rapuano}@unisannio.it

***Abstract* – The paper deals with the experimental comparison of two models for Analog-to-Information Converters (AICs). In particular, a *linear model in the time domain* and a *linear model in the frequency domain* have been considered and evaluated for the Random Demodulator AIC architecture. The aim of the present paper is (i) to evaluate the error introduced by both the AIC models, such to determine what best matches the actual implementation, and (ii) to determine the possible error in reconstructing the waveform due to the model.**

***Keywords* – Analog-to-Information Converter, Compressive Sampling, Random Demodulator, sub-Nyquist Sampling.**

I. INTRODUCTION

Traditional signal acquisition schemes are based on Shannon-Nyquist sampling theory, which indicates that the lowest sampling frequency of a band-limited analog signal should be at least equal to twice its bandwidth. However, in many applications, where the bandwidth of an analog signal is ultra-large, such as in radar detection and ultra-wideband communication, the traditional sampling schemes are difficult to be implemented 0. In fact, in typical applications, only a little fraction of the information carried by a signal of interest is relevant. The wideband signals in many RF applications have a large bandwidth but a small "*information rate*" [1]. In those cases, in order to reduce the sampling frequency, a new theory called Compressive Sampling (CS) has been proposed [3], by exploiting the sparse representation that many natural signals present.

CS proposes a new paradigm of acquisition that enables to merge in a single operation the sampling and compression phases, being an alternative approach to the traditional *sample-then-compress* paradigm, and allows to reliably reconstruct the signal of interest from a reduced number of samples, thus sparing sampling rate and acquisition memory. The basic idea of CS is to directly acquire the needed information in the sparse domain using lower sampling rate converters. A practical implementation of CS theory is done by Analog-to-Information Conversion (AIC) systems [4].

Current state-of-art research provides several hardware AIC architectures: random [5] or non-uniform sampling [6], random demodulation (RD) [7], random filter [8], random convolution [9], compressive multiplexer [10] and modulated wideband converter [11].

Most of the papers defining the AIC architectures also propose a mathematical model of that architecture, since it is needed to perform the waveform reconstruction from the compressed samples.

However, the capability of the AIC to acquire and recover the input signal depends on the adherence of the model to the actual implementation.

In particular, the greater the adhesion of the model to the implementation is, the greater is the AIC ability to reconstruct the input signal. Current research efforts are spent to characterize the non-idealities of each AIC block in order to improve the models. As an example, in [12] the non-idealities of the Pseudo-Random Binary Sequence (PRBS) are faced.

The purpose of this paper is to compare two models proposed for the RD AIC architecture. The analysis has been carried out on the RD architecture, as it is able to acquire wideband signals without the need of a wideband ADC. The models examined are a *linear model in the time domain*, proposed in [7] and a *linear model in the frequency domain*, proposed in [11]. In both cases the model can be represented by a linear transformation, either in the time or in the frequency domain [13].

The paper is structured as follows: Section II deals with the RD architecture. Section III illustrates the two models that have been compared. Section IV describes the experimental results that have been obtained by using the considered models.

II. AIC ARCHITECTURE

The block diagram of the RD-AIC is shown in Fig. 1. The

aim of this architecture is to compress an analog input signal into a much smaller bandwidth, which can be further sampled according to the Shannon theorem, encoding the signal information in a smaller set of samples.
It consists of four main system-level blocks: a PRBS generator, a mixer, an integrator (low-pass filter), a low-rate ADC.
The ADC is considered having a sampling frequency equal to f_s and the analog input signal $x(t)$, having a Nyquist frequency equal to $f_p = Kf_s$, with K positive integer greater than 1. Furthermore, $\mathbf{x} \in R^{Nx1}$ is defined as the vector of N samples of $x(t)$ if it was sampled by an ADC at a sampling frequency equal to f_p. Instead, $\mathbf{y}$ is the M-long vector of the AIC output, with $M < N$, representing the under-sampled version of $\mathbf{x}$.

Instead of directly sampling it, the input signal is mixed with a PRBS with values in the set {+1,-1}, called *chipping sequence p(t)*. The bit rate of the PRBS should be chosen not lower than f_p. Let's assume that it is equal to f_p and be $T_p = 1/f_p$.
In this case, $K = f_p / f_s$ defines the *sub-sampling factor*, which is equal to N/M. The bit rate f_p gives the maximum frequency component of the input signal that the AIC is able to acquire.
This mixing process allows to spread the harmonic content of the signal, so that at least some component of the mixed signal falls within the Nyquist band [0, $f_s/2$] of the ADC. The modulated output is then low-pass filtered and subsequently, by means of the A/D conversion, uniformly sampled at frequency f_s, lower than f_p. In this way, the information contained in the original signal has not been lost but mixed together in the baseband.
In the end, an estimate $\hat{\mathbf{x}}$ can be obtained by a suitable reconstruction algorithm from the elements of the vector $\mathbf{y}$ which represents an under-sampled version of $\mathbf{x}$.
In order to achieve good results in spreading the signal spectrum with the RD technique, in practice, it has been demonstrated that many parallel branches of mixers and integrators are needed [14].
This system, which modulates the input signal with multiple chipping sequence in parallel, is named Modulated Wideband Converter (MWC). It consists of m channels, driven by the same signal $x(t)$ where it is multiplied by a bank of j periodic waveforms $p_i(t)$, for i=1,…,j.

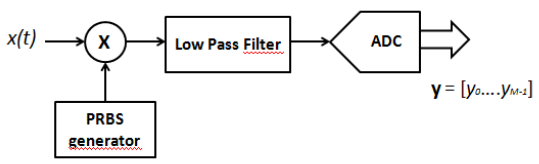

Fig. 1. Architecture of the random demodulation AIC.

III. AIC MODELS

A. Linear model in the time domain

According to the model suggested in [15][16], let indicate with [p_0, p_1, …, p_{N-1}] the samples of the PRBS. The mixing process can be modeled as the following matrix multiplication:

$$\mathbf{m} = \mathbf{P}\mathbf{x}. \tag{1}$$

where, $\mathbf{P}$ is the diagonal matrix, having the PRBS samples on the diagonal:

$$\mathbf{P} = \begin{bmatrix} p_0 & \cdots & 0 \\ \vdots & \ddots & \vdots \\ 0 & \cdots & p_{N-1} \end{bmatrix}. \tag{2}$$

The Low Pass Filter can be modeled by the Toeplitz matrix $\mathbf{H} \in R^{NxN}$, containing the impulse response of the filter:

$$\mathbf{H} = \begin{bmatrix} h_1 & h_2 & \cdots & h_{W-1} & 0 & \cdots & 0 \\ 0 & h_1 & \cdots & h_{W-2} & h_{W-1} & \cdots & 0 \\ \vdots & \vdots & \ddots & \vdots & \vdots & \cdots & \vdots \\ 0 & h_1 & \cdots & h_{W-2} & \cdots & h_{W-2} & h_{W-1} \end{bmatrix}, \tag{3}$$

where, $\mathbf{h}$ = [h_0, h_1,….,h_{W-1}] is the truncated impulse response of the low pass filter of length W≤N.
Finally, the compressed measurement vector $\mathbf{y}$ is obtained as:

$$\mathbf{y} = \mathbf{\Phi x} \tag{4}$$

where, $\mathbf{\Phi} \in R^{M \times N}$ is the measurement matrix that represents the model of the analog front-end of the random demodulator and it can be obtained by decimating the rows of the product $\mathbf{HP}$ by K. In this paper, the elements of the $\mathbf{\Phi}$ matrix have been obtained by means of a calibration phase.
In particular, N tests have been carried out, using the following signals as input:

$$x_i(t)=\cos(2\pi f_p/N) \quad i=0,\ldots,N/2, \tag{5}$$

$$x_i(t)=\sin(2\pi f_p/N) \quad i=N/2+1,\ldots,N-1, \tag{6}$$

and acquiring the AIC output $\mathbf{y}_i$ for each signal.
Then, $\mathbf{\Phi}$ has been evaluated as:

$$\mathbf{\Phi} = \mathbf{Y}\mathbf{X}^{-1} \tag{7}$$

where, $\mathbf{Y}$=[$\mathbf{y}_0$…$\mathbf{y}_{N-1}$] and $\mathbf{X}$=[$\mathbf{x}_0$….$\mathbf{x}_{N-1}$].

B. Linear model in the frequency domain

A linear model in the frequency domain can be obtained by adapting the model proposed in [11] for the MWC architecture, to the case of the RD.

In this case, the mixing process is modeled as a convolution in the frequency domain:

$$M(f) = X(f)*P(f). \quad (8)$$

where, *X(f)* is the Fourier transform of *x(t)*, defined as:

$$X(f) = \int_{-\infty}^{+\infty} x(t)e^{-j2\pi ft}\, dt, \quad (9)$$

and it is assumed zero for every $f \notin F = [1/2T_p, 1/2T_p)$.
P(f) is the Fourier transform of *p(t)*, where *p(t)* is a piecewise constant function that alternates between the levels ±1 for each of *N* equal time intervals. Formally,

$$p(t) = \alpha_k \quad kT_p \le t \le (k+1)T_p, \quad 0 \le k \le N-1 \quad (10)$$

with $\alpha_k \in \{+1,-1\}$, and $p(t + mNT_p) = p(t)$ for every $m \in Z$. Since *p(t)* is periodic, it has a Fourier expansion:

$$p(t) = \sum_{n=-\infty}^{\infty} p_n\, e^{j\frac{2\pi nt}{NT_p}} \quad (11)$$

where:

$$p_n = \frac{1}{NT_p}\int_0^{NT_p} p(t)e^{-\frac{j2\pi nt}{NT_p}}\, dt = \quad (12)$$

$$= \frac{1}{NT_p}\sum_{k=0}^{N-1} \alpha_k\, e^{-j\frac{2\pi nk}{N}} \int_0^{T_p} e^{-j\frac{2\pi nt}{NT_p}}\, dt. \quad (13)$$

Evaluating the integral, it is possible to define d_n as:

$$d_n = \frac{1}{NT_p}\int_0^{T_p} e^{-j\frac{2\pi nt}{NT_p}}\, dt = \begin{cases} \frac{1}{N} & n = 0 \\ \frac{1-\theta^n}{2j\pi n} & n \neq 0 \end{cases} \quad (14)$$

where, $\theta = e^{-j2\pi/N}$, and:

$$p_n = d_n \sum_{k=0}^{N-1} \alpha_k\, \theta^{nk}. \quad (15)$$

Thus, the Fourier transform *P(f)*, in terms of Fourier series coefficients p_n leads to:

$$P(f) = \sum_{n=-\infty}^{\infty} p_n \delta\left(f - \frac{n}{NT_p}\right), \quad (16)$$

with $\delta(t)$ denoting the Dirac delta function.
In [11], the Low Pass Filter *H(f)* is modeled to have a frequency response which is an ideal rectangular function:

$$H(f) = \mathrm{rect}\left(\frac{f}{f_s}\right), \quad (17)$$

with $\mathrm{rect}(x) = \begin{cases} 1 & if\ |x| < 1/2 \\ 0 & otherwise \end{cases}$.

In the case of this paper, the frequency response of the filter is not considered with a rectangular waveform. Instead, the filter used in the AIC prototype has been characterized in the frequency domain by generating sinewaves in the range $[0\text{-}f_p/2]$, with a step of f_p/N, considering f_p = 200 MSamples/s, directly to the input of the filter. Then, the output of the filter is acquired by the AD9230 Evaluation board and transferred to the computer by USB.
Finally, filtering *M(f)* by *H(f)*, the compressed measurement vector **y**, expressed in the discrete-time Fourier transform (DTFT) form, is obtained as:

$$Y(e^{j2\pi fT_s}) = \sum_{n=-L_0}^{+L_0} p_n\, X\left(f - \frac{n}{NT_p}\right) \quad (18)$$

with $f \in F$. L_0 is chosen as the smallest integer such that the sum contains all nonzero contributions of *X(f)* over *F*:

$$L_0 = \left\lceil \frac{f_p + f_s}{2f_p/N} \right\rceil - 1 = \left\lceil \frac{f_p + f_p\frac{M}{N}}{2f_p/N} \right\rceil - 1 = \left\lceil \frac{N+M}{2} \right\rceil - 1. \quad (19)$$

It is convenient to express (18) in matrix form, thus the digital output sequence becomes:

$$y(f) = \mathbf{sFDz}(f), \quad (20)$$

where, $y(f) = Y(e^{j2\pi fT_s})$, and $\mathbf{s} = [p_0 \ldots p_{N-1}]$. The *N* x *L* matrix **F**, with $L=2L_0+1$, is equal to:

$$\mathbf{F} = [\mathbf{G}_{L_0} \quad \ldots \quad \mathbf{G}_{-L_0}], \quad (21)$$

with:

$$\mathbf{G}_i = [\ \theta^{0\bullet i}, \theta^{2\bullet i}, \ldots\ldots, \theta^{(N-1)\bullet i}]^T \quad 0 < i < N-1. \quad (22)$$

The matrix **D** = $\mathrm{diag}(d_{L0}, \ldots, d_{-L0})$ is an L x L diagonal matrix with d_n defined by (14), and **z**(*f*) is a vector of length L, equal to:

$$\mathbf{z}(f) = [X(f - L_0 f_p), \ldots, X(f + L_0 f_p)]. \quad (23)$$

IV. EXPERIMENTAL RESULTS

A. Test strategy

All the reconstruction algorithms solve the problem (4) for given conditions. Therefore, the correctness of the reconstruction is heavily dependent from the capability of modeling **Φ** from the actual components used to realize the AIC in the sparse domain used to represent **y**.
The two considered models have been compared in terms of ***model error***.
This figure of merit is defined as:

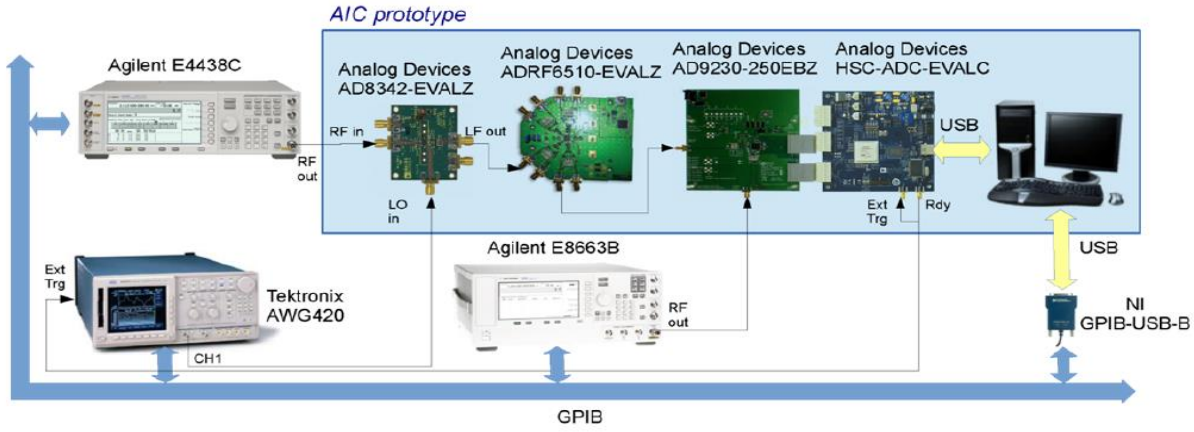

Fig. 2. Experimental setup used in the case of the random demodulation architecture [16].

$$\varepsilon_m = 20\log_{10}\frac{\sqrt{(y_{real}-y_{ideal})^2/M}}{\sqrt{y_{real}{}^2/M}}, \qquad (25)$$

where, y_{real} is the signal acquired from the AIC prototype, described in the following subsection and y_{ideal} is the signal evaluated according to each of the considered models. More in detail, y_{ideal} is obtained by following the steps described either in Section III.A for the model in the time domain, or in Section III.B, for the model in the frequency domain, considering a PRBS of length N = 512 samples.

Sinewave signals have been generated with frequencies in the range [5-95] MHz, with a step of 5 MHz. The PRBS has been generated with a bit rate of 200 Mbit/s. The sub-sampling factor K has been chosen equal to 1 or 4.

For the purpose of the tests, a MATLAB script has been designed to both control the instrumentation and evaluate the AIC models.

B. AIC prototype

The AIC prototype used for the tests is composed by an Analog Device AD8342 evaluation board that mixes the input signal with a PRBS (see Fig. 2).Then, the mixed signal is low-pass filtered by means of an Analog Devices ADRF6510 evaluation board. Such board contains an antialiasing filter with a cut-off frequency selectable in the range [1-30] MHz, which in this case is set to 19 MHz. After filtering, the signal is acquired by an Analog Device AD9230 evaluation board, containing a 12 bit ADC, operating at a sampling frequency of 50 MSamples/s.

Then, a HSC-ADC-EVALC Data Capture board allows the connection of the ADC evaluation board with the computer via a USB interface.

The input signal is generated by means of an Agilent E4438C Vector Signal Generator and the Agilent E8663B generator is used as sampling clock, while the PRBS is generated in the computer and downloaded, through the GPIB, to a Tektronix AWG420 Arbitrary Waveform Generator.

C. Results

The experiments have been conducted by considering 100 runs. In each plot of Figs. 3 to 5, the average of 100 results is reported.

In Fig. 3a, it is possible to observe the comparison between y_{ideal} and y_{real} for the *linear model in the time domain*, in the case of K = 4. It can be observed a good agreement between the model and the AIC outputs. The difference between the two signals, shown in Fig.3b showed a flat trend around zero.

In the Fig. 4, the error model is reported in decibel versus the frequency of the input sinewave signal, for K=1 and 4. It can be observed that the model error is almost constant with the frequency in both cases, around -23 dB

Regarding the *linear model in the frequency domain*, in Fig. 5a, the comparison of the y_{ideal} and y_{real} trends is reported, for K = 4. Compared with the other model, it can be seen that there are larger disagreements, that can be better appreciated in Fig. 5b, where the difference between the two signals is reported, and it showcases that the different is minimal.

In Fig. 6, the trend of the model error versus the frequency of the input signal is reported. It can be observed that, in the case of K=1, the error is almost constant around -18 dB. For K=4, the model error shows larger variations, with an average value of about -10dB.

It can be noted that the *linear model in the frequency domain* presents larger errors than the *linear model in the time domain*. This is mainly due to the fact that, in the latter case, the determination of the model parameters is done on the full path, thus including all the linear contributions in the whole chain from the input signal to the AIC output.

Instead, in the case of the *linear model in the frequency domain*, the low-pass filter has been characterized alone, and the mixer is modelled as a simple multiplication as specified in [10].

Moreover, in both cases the model error is high if

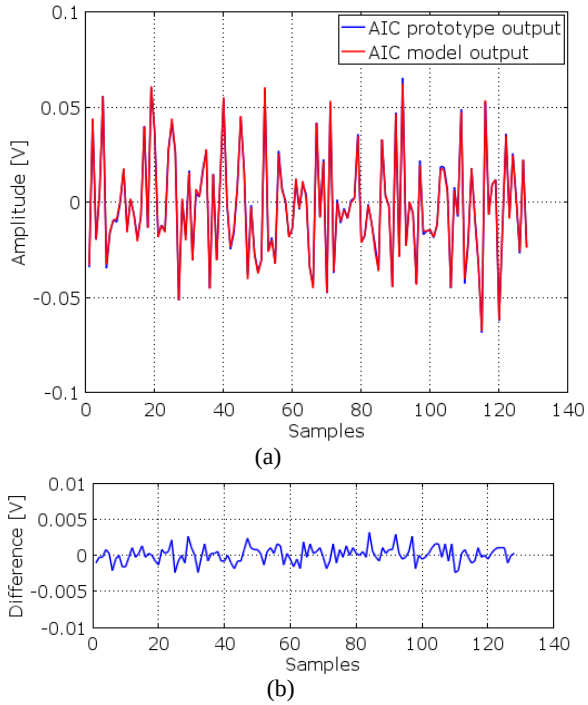

Fig. 3. Experimental result for test signal frequency at 5 MHz for K=4: comparison between y_{real} and y_{ideal} (a), and difference between y_{real} and y_{ideal} (b).

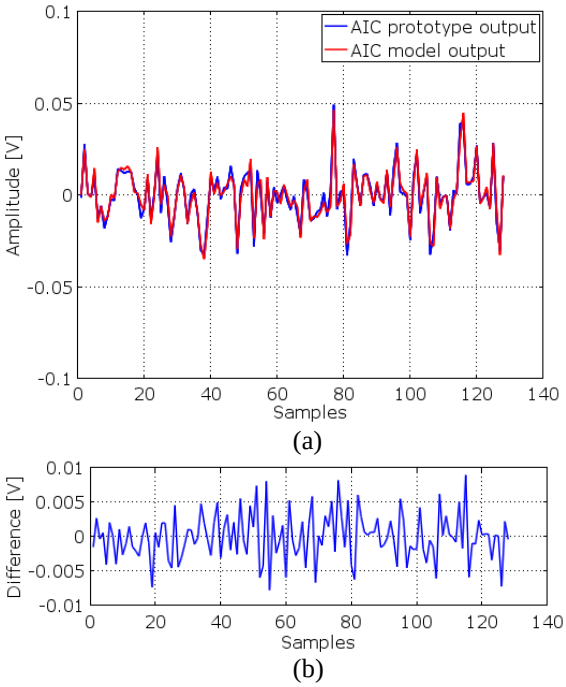

Fig. 5. Experimental result for test signal frequency at 5 MHz for K=4: comparison between y_{real} and y_{ideal} (a), and difference between y_{real} and y_{ideal} (b).

compared with the performances of an ADC, which, in the case of a 12 bit resolution, presents errors generally of the order of -60dB.

V. CONCLUSIONS

In this paper, an experimental evaluation of two AIC models has been carried out. It has been observed that both the considered models present huge model errors. This is due mainly to two reasons: (i) the linear model is not able to fully represent the behavior of the AIC, and in particular of the mixer, which is a highly non-linear device; (ii) even in the case of linear models, the determination of the model parameters is hard and highly depending on the calibration method used. Further work will be then concentrated to these two issues. In the former case, new models should be proposed, taking into account nonlinear behaviors. In the latter case, better procedures for the calibration will be explored, mainly in the case of the model in the frequency domain. In this case, as an example a calibration procedure involving the full path of the AIC could improve the accuracy of the parameter estimation.

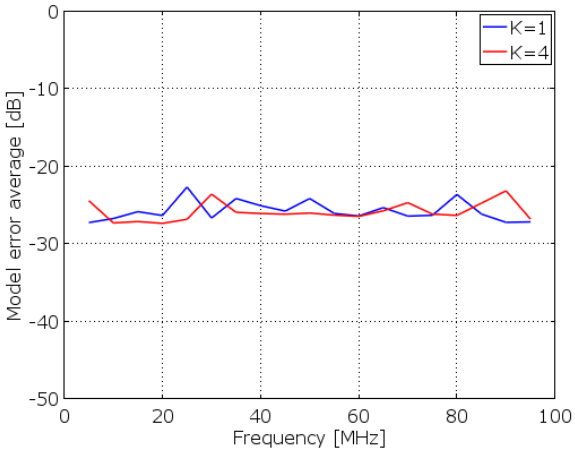

Fig. 4. Experimental results for test signal frequency range from 5 to 95 MHz, with a step of 5 MHz: *model error average* [dB], for K=1 and K=4.

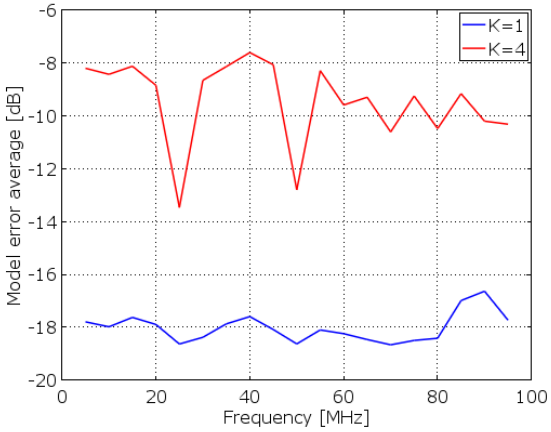

Fig. 6. Experimental results for test signal frequency range from 5 to 95 MHz, with a step of 5 MHz: *model error average* [dB], for K=1 and K=4.

REFERENCES

[1] P.Daponte, S.Rapuano, L.De Vito, I.Tudosa, "Challenges for aerospace measurement systems: Acquisition of wideband radio frequency using Analog-to-Information converters", Proceedings of the IEEE International Workshop on Metrology for Aerospace, pp. 377–382, 2014.

[2] M.Vetterli, P.Marziliano, and T.Blu, "Sampling signals with finite rate of innovation", IEEE Transactions on Signal Processing, vol.50, No.6, pp. 1417-1428, June 2002.

[3] E.J.Candès, "Compressive sampling",Proceedings of the International Congress of Mathematicians,vol. 3, pp.1433-1452, 2006

[4] S.Rapuano "Analog-to-Information Converters: research trends and open problems", Proc. of 26th Conference Radioelektronika, Košice, pp.10-17, April 2016.

[5] J.Laska, S.Kirolos, "Random sampling for analog-to-Information conversion of wideband signals", Proc. of IEEE Dallas/CAS Workshop on Design, Applications, Integration and Software, Oct. 2006, pp.119-122

[6] M.Walkin, S.becker, E.Nakamura, M.Grant, E.Sovero, D.Ching, J.Yoo, J.Romberg, A.Emami-Neyestanak, E.Candes, "A Nonuniform Sampler for Wideband Spectrally-Sparse Environments", IEEE Journal on Emerging and Selected Topics in Circuits and Systems, vol.2, No.3, pp.516-529, Sept. 2012.

[7] S.Kirolos, J.Laska, M.Wakin, M.Duarte, D.Baron, T.Ragheb, Y.Massoud, R.Baraniuk, "Analog-to-Information Conversion via Random Demodulation", Proc. of 2006 IEEE Dallas/CAS Workshop on Design, Applications, Integration and Software, Oct. 2006, pp.71-74.

[8] J.Tropp, M.Wakin, M.Duarte, D.Baron, R.Baraniuk, "Random Filters for Compressive Sampling and Reconstruction", Proceedings of IEEE International Conference on Acoustic Speed and Signal Processing, vol.3, pp.III-872-III-875.

[9] J.Romberg, "Compressive sensing by random convolution", SIAM Journal on Imaging Sciences, vol.2, No.4, pp. 1098-1128, 2009

[10] J.P. Slavinsky, J.N. Laska, M.A. Davenport and R.G. Baraniuk, "The compressive multiplexer for multi-channel compressive sensing", Proc. of 2011 IEEE Int. Conf. Acoust., Speech Signal. (ICASSP), Prague, Czech Republic, 2011, pp. 3980-3983

[11] M. Mishali, Y.C. Eldar, "From theory to practice: sub-Nyquist sampling of sparse wideband analog signals", IEEE J.Sel. Topics Signal Process, vol. 4, no. 2, pp. 375-391, 2010

[12] P.Daponte, L.De Vito, G.Iadarola, S.Rapuano "PRBS non-idealites affecting Random Demodulation Analog-to-Information converters", Proceedings of 19th Internationl Workshop on ADC Modelling and Testing, Budapest, Hungary, Sept. 2016.

[13] P.Daponte, L.De Vito, G.Iadarola, S.Rapuano "Effects of PRBS jitter on random demodulation Analog-to-Information Converters", Proceedings of the 3rd IEEE International Workshop on Metrology for Aerospace, Florence, Italy, June 2016, pp. 643-648.

[14] M.Mishali, Y.C.Eldar, "Xampling: analog data compression", Proc. of Data Compression Conference, 24-26 March 2010, Snowbird, Utah, USA, pp.366-375.

[15] Pawel J.Pankiewicz, Thomas Arildsen, Torben Larsen, "Sensivity of the random demodulation framework to filter tolerances", European Signal Processing Conference (EUSIPCO), Barcelona, 2011

[16] D.Bao, P.Daponte, S.Rapuano, L.De Vito, "Frequency domain characterization of random demodulation analog to information converters", ACTA IMEKO, vol. 4, pp. 111-120, 2015.